Icarus 264 (2016) 465–477

Contents lists available at ScienceDirect

Icarus

journal homepage: www.journals.elsevier.com/icarus

The solsticial pause on Mars: 2 modelling and investigation of causes

David P. Mulholland [a,*], Stephen R. Lewis [b], Peter L. Read [a], Jean-Baptiste Madeleine [c], Francois Forget [c]

[a] Atmospheric, Oceanic & Planetary Physics, University of Oxford, Clarendon Laboratory, Parks Road, Oxford OX1 3PU, UK
[b] Department of Physical Sciences, The Open University, Walton Hall, Milton Keynes MK7 6AA, UK
[c] Laboratoire de Météorologie Dynamique (LMD), CNRS, IPSL, 4 pl. Jussieu, 75252 Paris, France

ARTICLE INFO

Article history:
Received 16 April 2015
Revised 29 July 2015
Accepted 7 August 2015
Available online 21 September 2015

Keywords:
Mars, atmosphere
Mars, climate
Atmospheres, dynamics

ABSTRACT

The martian solsticial pause, presented in a companion paper (Lewis et al., 2016), was investigated further through a series of model runs using the UK version of the LMD/UK Mars Global Climate Model. It was found that the pause could not be adequately reproduced if radiatively active water ice clouds were omitted from the model. When clouds were used, along with a realistic time-dependent dust opacity distribution, a substantial minimum in near-surface transient eddy activity formed around solstice in both hemispheres. The net effect of the clouds in the model is, by altering the thermal structure of the atmosphere, to decrease the vertical shear of the westerly jet near the surface around solstice, and thus reduce baroclinic growth rates. A similar effect was seen under conditions of large dust loading, implying that northern midlatitude eddy activity will tend to become suppressed after a period of intense flushing storm formation around the northern cap edge. Suppression of baroclinic eddy generation by the barotropic component of the flow and via diabatic eddy dissipation were also investigated as possible mechanisms leading to the formation of the solsticial pause but were found not to make major contributions. Zonal variations in topography were found to be important, as their presence results in weakened transient eddies around winter solstice in both hemispheres, through modification of the near-surface flow. The zonal topographic asymmetry appears to be the primary reason for the weakness of eddy activity in the southern hemisphere relative to the northern hemisphere, and the ultimate cause of the solsticial pause in both hemispheres. The meridional topographic gradient was found to exert a much weaker influence on near-surface transient eddies.

1. Introduction

In Lewis et al. (2016), hereafter referred to as P1, martian transient waves were diagnosed from a reanalysis of Thermal Emission Spectrometer (TES) data. A particular feature identified in the record was the 'solsticial pause': a weakening of waves near the surface around winter solstice of each year analysed, seen in both hemispheres.

Solsticial pauses with a range of depths have been simulated by martian global climate models (MGCMs) (Hourdin et al., 1995; Basu et al., 2006; Wang et al., 2013; Kavulich et al., 2013), and existing modelling literature suggests that the depth of a modelled solsticial pause is enhanced by the presence of one or both of a large solsticial dust loading (representative of a global dust storm) (Hourdin et al., 1995; Kuroda et al., 2007) and radiatively active water ice clouds (Wilson, 2011). The reduction in eddy activity under conditions of high dust loading is understood to be a result of changes to the zonal jet (Kuroda et al., 2007), and several important features of winter hemisphere eddies have been drawn from observational data (Wang, 2007), but a detailed description of the mechanisms behind the solsticial pause, which occurs during years both with and without a global dust storm, is currently lacking.

The midwinter minimum in North Pacific atmospheric storminess on Earth, though different in several ways to the martian solsticial pause (see P1), has been studied in detail in recent years, and some of the explanations put forward for the terrestrial case may be relevant to Mars. These include: an increase in barotropic damping around solstice (Deng and Mak, 2006); eddy dissipation through diabatic effects (Chang, 2001); and localised effects of interaction with topography (Penny et al., 2010; Park et al., 2010).

In this paper we use an MGCM to measure the net effects of several of these factors, some of which may contribute to the formation of the pause, in both hemispheres. First, in Section 2, the model used is described. In Section 3, the set of simulations are introduced, along with summary measures of the extent to which

* Corresponding author at: Department of Meteorology, University of Reading, Harry Pitt Building, Reading RG6 6AL, UK.
E-mail address: d.p.mulholland@reading.ac.uk (D.P. Mulholland).

http://dx.doi.org/10.1016/j.icarus.2015.08.038
0019-1035/

each is able to reproduce solsticial minima similar to those shown in P1. Section 4 analyses the contributions of various mechanisms to the formation of the solsticial pause, from seasonal variation in atmospheric baroclinicity, to other means of reducing eddy growth, and finally to the more fundamental impact of surface topography. In Section 5, the role of topography is discussed further, and our insights into the nature of the pause are used to provide explanation for its interannual variability as presented in P1. Finally, the key results of the paper are summarised in Section 6.

2. Model description

The model used from this study is an updated, UK version of the LMD/UK Mars Global Climate Model (UKMGCM) described in P1. This version includes a microphysical cloud scheme, which predicts ice particle sizes and growth rates taking into account temperature, humidity and local density of dust nuclei (Montmessin et al., 2004; Madeleine et al., 2012). Water vapour and ice tracers undergo parameterised turbulent diffusion, convective adjustment and gravitational sedimentation. The radiative effect of water ice clouds can be included; the radiation scheme (Madeleine et al., 2011) calculates cloud extinction depending on the ice particle size, using optical parameters from Warren (1984) (see Madeleine et al. (2012) for more details).

Full lifting and transport simulations using radiatively active dust are possible in the UK model, but in this work, prescribed dust opacities are used in lieu of a transported dust field, to enable more direct comparisons with observations and to fix the dust opacity field within a set of controlled model experiments used to study the sensitivity of the solsticial pause to several different effects. In this mode, the dust field that the radiation scheme 'sees' is comprised of particles of radius 1.5 μm, with variation of mass mixing ratio with height following a Conrath profile. Mixing ratios are scaled so that the total column optical depth, calculated in two visible/near-IR bands and three thermal IR bands and using a ratio of visible to infrared opacity of 2, fits a prescribed distribution. The visible optical depth may have a constant value in time and space, or follow a more complex spatially and/or temporally varying function (Forget et al., 1999).

One such distribution used in this work varies with longitude, latitude and time, and replicates dust opacities from MY24 as observed by the Thermal Emission Spectrometer onboard Mars Global Surveyor (Smith et al., 2000). It was constructed using the reanalysis dataset described in P1. Since data were not available for L_s = 0–140° in MY24, the dust opacity scenario for this year uses optical depths from MY25 of the reanalysis dataset during this period. The differences in dust loading between years is expected to be fairly small at this time of the martian year (northern spring/summer). The 'MY24' dust scenario is shown as a zonal mean in Fig. 1.

The key point is that model runs using the 'MY24' scenario can be compared directly to the reanalysis. Aside from possible inaccuracies in the vertical dust distribution, which will be compensated for in the reanalysis (through temperature assimilation) but not in the free-running model, any differences between model and reanalysis represent deficiencies in the model's ability to simulate correctly the atmospheric state (temperature, pressure, wind) given the correct dust opacity forcing.

Note that there is considerable uncertainty in the column dust opacity in both winter polar regions, as there were no TES opacity data available in these regions. As a result of the approach taken in the data assimilation procedure, dust opacities remain constant over a period without available observations, as can be discerned from Fig. 1. The simulations presented in the next section include the use of two alternative prescribed dust distributions, which gives information on the sensitivity to dust loading more generally,

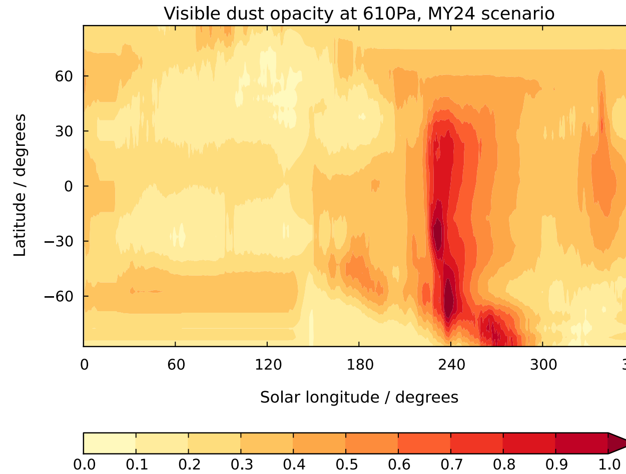

Fig. 1. The 'MY24' dust scenario, constructed from a combination of MY24 and MY25 reanalysis dust opacities, plotted as a zonal mean function of latitude and solar longitude.

and provides some confidence that the impact of water ice clouds is not specific to the use of a particular, possibly inaccurate, polar dust distribution.

The model runs described below were all carried out using the T31 spectral truncation, corresponding to a 3.75°×3.75° dynamical grid and a 5°×5° physics grid, the same as was used for the reanalysis of P1. The use of a free-running MGCM complements the analysis of observational and assimilated data by allowing the isolation of the net effects of each of several physical mechanisms, through the use or neglect of each in a particular simulation. In this work, the three model forcings that were varied in this way were the dust opacity field, the radiative effects of water ice clouds and the surface topography.

3. Model simulations

To test whether or not the model reproduces the reanalysis as presented in P1, and to investigate the conditions necessary for the formation of a solsticial pause, a series of simulations were performed using, in each case, a prescribed dust opacity field. The simulations are named and summarised in Table 1. Two used the 'MY24' dust scenario described previously, one including the radiative effects of water ice clouds (τ^*_{MY24}) and the other neglecting clouds (τ_{MY24}). A similar pair of runs with (τ^*_{low}) and without (τ_{low}) clouds used instead a constant visible dust opacity of 0.2, referenced to the 610 Pa pressure surface. Finally, τ_{high} simulated a large, perennial dust storm by using a constant 610 Pa dust opacity of 2.0, and neglected water ice clouds.

Table 1 also includes a quantity $\frac{[T'_{max}]_{solstice}}{[T'_{max}]_{pre,post}}$ (along with its constituent parts) which measures, in a crude way, the extent to which a solsticial pause was produced in the northern hemisphere for a

Table 1
Summary of the model simulations performed.

Name	Dust opacity	Clouds?	$[T'_{max}]_{solstice}$	$[T'_{max}]_{pre,post}$	$\frac{[T'_{max}]_{solstice}}{[T'_{max}]_{pre,post}}$
τ_{MY24}	MY24	No	6.40	7.09	0.90
τ^*_{MY24}	MY24	Yes	5.55	7.94	0.70
τ_{low}	0.2	No	7.91	7.42	1.07
τ^*_{low}	0.2	Yes	8.39	9.18	0.91
τ_{high}	2.0	No	5.51	7.27	0.76
MY24 reanalysis			3.35	6.72	0.50